energies

MDPI

Article

Dimensionless Impedance Method for General Design of Surge Tank in Simple Pipeline Systems

Sanghyun Kim [1,*] and Dooyong Choi [2]

[1] Department of Environmental Engineering, Pusan National University, 2, Busandaehak-ro 63beon-gil, Geumjung-gu, Busan 46241, Korea
[2] K-Water Institute, 125 Yuseong-daero, Daeheon 34045, Korea; dooyong@kwater.or.kr
* Correspondence: kimsangh@pusan.ac.kr; Tel.: +82-51-510-2479

Abstract: The design of surge protection devices is a practical issue for the management of pressurized pipeline systems. Depending on the flow status, dimension, material, and fluid properties of a particular pipeline, the generation of hydraulic transients and their interactions with surge protection devices have been explored considering different conditions for various pipeline systems. The resonance between the pipeline elements and surge energy absorption function of the hydraulic structure should be adaptively considered for each pipeline system. To comprehensively address surge generation and surge alleviating process, this study introduced dimensionless equations of fluid motion and continuity, and their solutions were developed in the dimensionless frequency domain. The impact of the surge tank, pressure accumulator, and its connector were also developed in terms of dimensionless operators. The impact of distinct flow conditions and pipeline properties was successfully addressed by an integrated parameter, dimensionless resistance, which also provided a unified condition for water hammer similarity in reservoir pipeline surge tank pipeline valve (RPSPV) systems. The development of dimensionless hydraulic impedance expressions along a pipeline system and its conversion into a response function provides a normalized pressure response in the dimensionless time domain. Excellent agreement was found between transient simulations using the developed method and those obtained using existing methods. The integration of a dimensionless approach into a metaheuristic engine provides a general platform for surge tank (ST) design in the comprehensive bounds of flow and pipeline conditions.

Keywords: dimensionless surge tank design; pipeline systems; dimensionless impedance method; similarity in hydraulic transient

check for updates

Citation: Kim, S.; Choi, D. Dimensionless Impedance Method for General Design of Surge Tank in Simple Pipeline Systems. *Energies* **2022**, *15*, 3603. https://doi.org/10.3390/en15103603

Academic Editor: Helena M. Ramos

Received: 22 March 2022
Accepted: 12 May 2022
Published: 14 May 2022

1. Introduction

Surge-arresting devices have frequently been used to protect structures along pipeline systems from water hammers generated by sudden valve actions or the starting or stopping of pumping stations. Rapid variations in flow velocity introduce a sudden generation of pressure waves, which propagate and bounce back along the pipelines. Both overpressure and underpressure in transient events, such as a sudden burst of pipeline elements or cavitation resulting from column separation, can damage pipeline systems. Various hydraulic devices such as surge tanks, air chambers, and pressure relief valves are usually installed close to the flow control valves or pumping stations. The method of characteristics (MOC) has been widely used to predict hydraulic transients in pipeline systems [1]. The design of surge tanks and air vessels has been focused on obtaining the optimum dimensions of the structure in the context of transient analysis [2–6]. Surge tank analysis, design, stability analysis, and optimization have also been explored based on several discretization platforms (i.e., the finite difference method and finite element method) [7–10]. As an alternative to discretization approaches, the impulse response method (IRM) has demonstrated the potential of the frequency domain approach as an alternative method for the design of hydraulic structures with transient analysis [11].

The surge issue in pipeline systems tends to be pronounced for a simple pipeline valve system (such as a water supply system) because the impact of surge can be critical for a system with no diverting structures, such as loops and branches, to mitigate the water hammer impact through the divergence of the pressure wave pathway. The impact of surge arrest devices on complex pipe networks has been explored using several modeling approaches [12,13]. Furthermore, the optimization of an air chamber or valve for transient protection has been performed to achieve various objective functions [14–16].

The design of optimum parameters for the surge tank or air chamber depends on the physical characteristics of the system (e.g., pipeline length, diameter, materials, and wall thickness) and hydraulic conditions (e.g., flow rate and surge introducing driver). However, the fundamental principles of surge generation, propagation, and mitigation processes are identical for different pipeline systems. Even though a common layout of the water supply system as a reservoir pipeline surge tank pipeline valve (RPSPV) is widely used, universal design and performance prediction for surge protection devices is difficult to achieve because each system has different flow and transient response features, which are determined by distinct system characteristics. Numerous studies have been conducted on designing the dimensions of surge protection devices by combining the solutions of the hydraulic governing equation and metaheuristic approaches [8,11,13]; however, an efficient, holistic approach can be introduced if the dimension issue of RPSPV systems is properly addressed. In other words, if the units of all physical quantities can be neutralized in motion and continuity equilibrium, then a general simulation and comparison between different systems can be achieved in a universal context.

The governing equations and their solutions were developed based on dimensionless space. The three objectives of this study were as follows:

1. Dimensionless differential equations for mass and momentum conservation were developed for pipeline systems with surge protection devices.
2. Solutions for dimensionless governing equations were developed in terms of operators such as the dimensionless hydraulic impedance and propagation constant through linearization and integration in the dimensionless frequency domain.
3. The dimensionless time-domain response functions were integrated into a widely used optimization scheme, particle swarm optimization (PSO), to delineate a comprehensive solution for surge tank design in RPSPV systems.

2. Materials and Methods

2.1. Dimensionless Equations for Hydraulic Transient in Pipeline Systems

Unsteady variations in the pressure head and flow rate in pressurized pipeline systems can be described by differential equations of continuity and momentum conservation, which can be expressed as follows [1]:

$$\frac{\partial Q}{\partial t} + gA\frac{\partial H}{\partial x} + \frac{fQ|Q|}{2DA} = 0 \tag{1}$$

$$\frac{a^2}{gA}\frac{\partial Q}{\partial x} + \frac{\partial H}{\partial t} = 0 \tag{2}$$

where Q is the mean flow rate, H is the piezometric head, a is the wave propagation speed, g is the gravitational acceleration, x is the distance, t is the time, f is the Darcy–Weisbach friction factor, and D is the diameter.

Considering an RPSPV system shown in Figure 1, Equations (1) and (2) can be converted into the dimensionless equation, as dependent variables were transformed into dimensionless dependent variables as follows: $H = 4a'Q_{0r}/\left(g\pi D'^2\right)\hat{H}$ and $Q = Q_{0r}\hat{Q}$, where a' is the wave speed in the main pipeline, D' is the diameter in the main pipeline, and Q_{0r} is the reference steady flow rate. Independent variables can be transformed into dimensionless forms as follows: $t = L'/a'\hat{t}$ and $x = L'\hat{x}$, where L' is the main pipeline length.

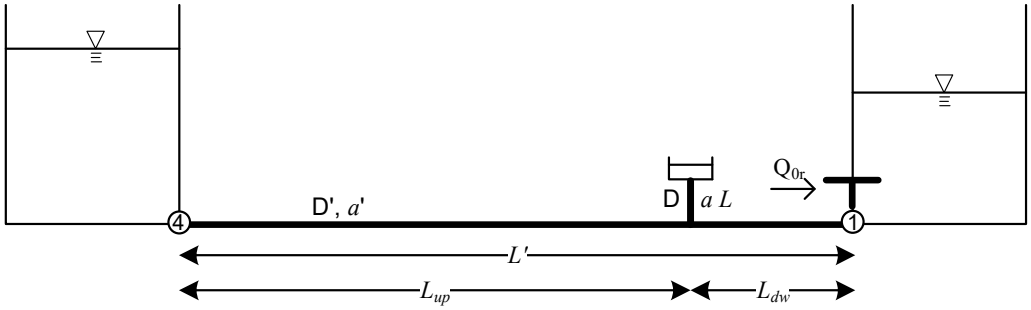

Figure 1. RPSPV system schematic.

For the dimensionless variables $L_r = L/L'$, $a_r = a/a'$, and $D_r = D/D'$, the dimensionless continuity and momentum equations can be expressed as follows:

$$\frac{\partial \hat{Q}}{\partial \hat{t}} + {D_r}^2 \frac{\partial \hat{H}}{\partial \hat{x}} + \frac{f Q_{0r} |Q_{0r}|}{2DA} \frac{L a_r}{L_r a Q_{0r}} = 0 \tag{3}$$

$$\frac{\partial \hat{H}}{\partial \hat{t}} + \frac{{a_r}^2}{{D_r}^2} \frac{\partial \hat{Q}}{\partial \hat{x}} = 0 \tag{4}$$

The dimensionless parameters, D_r, L_r, and a_r are one of the main parts of the RPSPV system, and Equations (3) and (4) can be expressed in a simpler form. The dimensionless flow rate and pressure head can be decomposed into their mean and perturbation components as follows: $\hat{H} = \overline{\hat{H}} + \hat{h}'$ and $\hat{Q} = \overline{\hat{Q}} + \hat{q}'$, and the dimensionless perturbation equations for the main pipeline element can be expressed as follows:

$$\frac{\partial \hat{h}'}{\partial \hat{x}} + \frac{\partial \hat{q}'}{\partial \hat{t}} + \hat{R}\hat{q}' = 0 \tag{5}$$

$$\frac{\partial \hat{h}'}{\partial \hat{t}} + \frac{\partial \hat{q}'}{\partial \hat{x}} = 0 \tag{6}$$

where the dimensionless resistance $\hat{R} = fL'Q_{or}/(2DA'a')$ for the turbulent flow condition and $\hat{R} = V_{or}D/(128\nu a')$ for the laminar flow condition, where A' is the cross-sectional area of the main pipeline and ν is the dynamic viscosity.

Combining Equations (5) and (6) into a function of $\hat{q}'$ can be expressed as follows:

$$\frac{\partial^2 \hat{q}'}{\partial \hat{t}^2} + \hat{R}\frac{\partial \hat{q}'}{\partial \hat{t}} = \frac{\partial^2 \hat{q}'}{\partial \hat{x}^2} \tag{7}$$

Further development of Equations. (5)–(7) provide expressions for $\hat{h}'$ as follows:

$$\frac{\partial^2 \hat{h}'}{\partial \hat{t}^2} + \hat{R}\frac{\partial \hat{h}'}{\partial \hat{t}} = \frac{\partial^2 \hat{h}'}{\partial \hat{x}^2} \tag{8}$$

It is assumed that the pressure head fluctuation $\hat{h}'$ is decomposed into a function of the dimensionless distance $(\hat{x})$ and dimensionless time $(\hat{t})$ as follows:

$$\hat{h}' = X(\hat{x})T(\hat{t}) \tag{9}$$

Introducing two spatial propagation characteristics and a time-marching feature for dimensionless space and time terms as follows: $X(\hat{x}) = A_1 e^{\hat{\gamma}\hat{x}} + A_2 e^{-\hat{\gamma}\hat{x}}$ and $T(\hat{t}) = A_3 e^{\hat{s}\hat{t}}$, where $\hat{s}$ is the dimensionless frequency, and the dimensionless propagation constant $\hat{\gamma}$ can be expressed as follows:

$$\hat{\gamma} = \sqrt{\hat{s}(\hat{s} + \hat{R})} \tag{10}$$

The dimensionless pressure head and discharge can be expressed as follows:

$$\hat{H}(x) = C_1 e^{\hat{\gamma}\hat{x}} + C_2 e^{-\hat{\gamma}\hat{x}} \tag{11}$$

$$\hat{Q}(x) = -\frac{1}{\hat{Z}_c}\left(C_1 e^{\hat{\gamma}\hat{x}} - C_2 e^{-\hat{\gamma}\hat{x}}\right) \tag{12}$$

where $\hat{Z}_c = \hat{\gamma}/\hat{s}$ is the dimensionless characteristic impedance and C_1 and C_2 are integration constants.

By evaluating constants C_1 and C_2 using the upstream boundary condition, the general dimensionless relationship between the upstream and downstream dimensionless pressure heads ($\hat{H_U}$, $\hat{H_D}$) and flow rates ($\hat{Q_U}$, $\hat{Q_D}$) can be expressed as follows:

$$\hat{H_D} = \hat{H_U}\cos h\hat{\gamma}\hat{x} - \hat{Z}_c\hat{Q_U}\sin h\hat{\gamma}\hat{x} \tag{13}$$

$$\hat{Q_D} = -\frac{\hat{H_U}}{\hat{Z}_c}\sin h\hat{\gamma}\hat{x} + \hat{Q_U}\cos h\hat{\gamma}\hat{x} \tag{14}$$

2.2. Connecting Pipeline Element for Surge Tank

The dimensionless perturbation equations for connecting the pipeline elements of the surge tank can be expressed as follows:

$$\frac{\partial \hat{h}'}{\partial \hat{t}} + \frac{{a_r}^2}{{D_r}^2}\frac{\partial \hat{q}'}{\partial \hat{x}} = 0 \tag{15}$$

$${D_r}^2\frac{\partial \hat{h}'}{\partial \hat{x}} + \frac{\partial \hat{q}'}{\partial \hat{t}} = 0 \tag{16}$$

Combining Equations (15) and (16) into a function of the perturbation dimensionless flow rate can be expressed as follows:

$$\frac{\partial^2 \hat{q}'}{\partial \hat{t}^2} = {a_r}^2\frac{\partial^2 \hat{q}'}{\partial \hat{x}^2} \tag{17}$$

Further development of Equations (15) and (16) for $\hat{h}'$ can be expressed as follows:

$$\frac{\partial^2 \hat{h}'}{\partial \hat{t}^2} = {a_r}^2\frac{\partial^2 \hat{h}'}{\partial \hat{x}^2} \tag{18}$$

Introduction of Equation (9), with a similar development of the main pipeline into the connecting pipeline element, the dimensionless propagation constant for the connecting element $\hat{\gamma}_c$ can be expressed as follows:

$$\hat{\gamma}_c = \sqrt{\frac{\hat{s}^2}{{a_r}^2}} \tag{19}$$

Therefore, the dimensionless pressure head and discharge for the connecting pipeline element can be expressed as follows:

$$\hat{H}(x) = {C_1}' e^{\hat{\gamma}_c\hat{x}} + {C_2}' e^{-\hat{\gamma}_c\hat{x}} \tag{20}$$

$$\hat{Q}(x) = -\frac{1}{\hat{Z_{cc}}}\left({C_1}' e^{\hat{\gamma}_c\hat{x}} - {C_2}' e^{-\hat{\gamma}_c\hat{x}}\right). \tag{21}$$

where $\hat{Z_{cc}} = \left(\hat{\gamma}_c {a_r}^2\right)/\left(\hat{s}{D_r}^2\right)$ is the dimensionless characteristic impedance, and ${C_1}'$. and ${C_2}'$ are integration constants.

Based on the derived general dimensionless relationship between the upstream surge tank and downstream location x, the dimensionless pressure heads ($\hat{H_{ST}}$, $\hat{H}_x$) and flow rates ($\hat{Q_{ST}}$, $\hat{Q}_x$) can be expressed as follows:

$$\hat{H}_x = \hat{H_{ST}}\cos h\hat{\gamma}_c\hat{x} - \hat{Z_{cc}}\hat{Q_{ST}}\sin h\hat{\gamma}_c\hat{x} \tag{22}$$

$$\hat{Q}_x = -\frac{\hat{H_{ST}}}{\hat{Z_{cc}}}\sin h\hat{\gamma}\hat{x} + \hat{Q_{ST}}\cos h\hat{\gamma}_c\hat{x} \tag{23}$$

2.3. Dimensionless Hydraulic Impedance at Surge Tank

The pressure head fluctuation of the surge tank was approximated as $h' = H_{ST}e^{i\omega t}$ and its flowrate fluctuation was calculated as $q' = -A_s dh'/dt$, where H_{ST} is the pressure head at the surge tank and A_s is the surge tank area [1].

Introducing dimensionless dependent variables as $h' = (a'Q_{or})/(gA')\hat{h}'$ and $q' = Q_{0r}\hat{q}'$, where A' is the cross-sectional area of the main pipeline, and the dimensionless independent variables as $t = L'/a'\hat{t}$ and $\omega = a'/L'\hat{s}$, the dimensionless head fluctuation can be expressed as follows:

$$\hat{h}' = \hat{H}e^{i\hat{s}\hat{t}} \tag{24}$$

where $\hat{H} = (gA'H_{ST})/(a'Q_{0r})$.

The dimensionless flow rate fluctuation can be expressed as follows:

$$\hat{q}' = \hat{Q}e^{i\hat{s}\hat{t}} \tag{25}$$

where $\hat{Q} = -A_{sr}(a'A'H_{ST})/(gL'Q_{0r})i\hat{s}$, where $A_{sr} = A_s/A'$.

Therefore, the dimensionless hydraulic impedance at the surge tank can be expressed as follows:

$$\hat{Z_{ST}} = \frac{gL'i}{A_{sr}a'^2\hat{s}} \tag{26}$$

2.4. Dimensionless Hydraulic Impedances for RPSPV System

As shown in Figure 1, the schematic for the RPSPV system can be converted into a dimensionless system by introducing dimensionless variables as follows: $\hat{x_{up}} = L_{up}/L'$, $\hat{x_{dw}} = L_{dw}/L'$, and $\hat{x_c} = L/L'$.

The hydraulic impedance of the main pipeline upstream of the connecting element can be approximated as follows:

$$\hat{Z}_{uc}(\hat{x}) = -\hat{Z}_c\tanh\hat{\gamma}\hat{x_{up}} \tag{27}$$

where $\hat{Z}_c(\hat{x}) = \hat{\gamma}/\hat{s}$, and $\hat{\gamma} = \sqrt{\hat{s}(\hat{s}+\hat{R})}$.

Considering the hydraulic impedance at the surge tank, the hydraulic impedance downstream of the connecting element can be expressed as follows:

$$\hat{Z}_{cc}(\hat{x_c}) = \frac{\hat{Z_{ST}} - \hat{Z_{cc}}\tanh\hat{\gamma_{cc}}\hat{x_{cc}}}{1 - \hat{Z_{ST}}/\hat{Z_{cc}}\tanh\hat{\gamma_{cc}}\hat{x_{cc}}} \tag{28}$$

where $\hat{Z_{cc}} = \left(\hat{\gamma_{cc}}{a_r}^2\right)/(\hat{s}D_r)$, and $\hat{r_{cc}} = \sqrt{\hat{s}^2/{a_r}^2}$.

If the size of the surge tank is sufficiently large, then the head variation in the surge tank can be ignored, and the hydraulic impedance downstream of the connecting element can be simplified as follows:

$$\hat{Z}_{cc}(\hat{x_c}) = -\hat{Z_{cc}}\tanh\hat{\gamma_{cc}}\hat{x_{cc}} \tag{29}$$

The hydraulic impedance of the main pipeline downstream of the connecting element can be evaluated as follows:

$$\hat{Z_{dc}}(\hat{x}) = \frac{-\hat{Z}_c \tanh\hat{\gamma}\hat{x_{up}}}{1 - \hat{Z}_c \tanh\hat{\gamma}\hat{x_{up}}/\hat{Z_{cc}}(\hat{x_c})} \tag{30}$$

Therefore, the hydraulic impedance at the downstream valve can be expressed as follows:

$$\hat{Z_{dv}}(\hat{x}) = \frac{\hat{Z_{dc}}(\hat{x}) - \hat{Z}_c \tanh\hat{\gamma}\hat{x_{dw}}}{1 - \hat{Z_{dc}}(\hat{x})/\hat{Z}_c \tanh\hat{\gamma}\hat{x_{dw}}} \tag{31}$$

The Fourier transformation (e.g., fast Fourier transformation) of Equation (30) provides the response function in the dimensionless time domain, which can be used to obtain the dimensionless pressure response at a designated point in the RPSPV system.

2.5. Dimensionless Lumped Inertia

Lumped inertia can be applied to low-frequency oscillations in short pipelines and short risers in surge tanks [1]. The relationship of the pressure head in the downstream and upstream flow rates can be written as follows:

$$H_D = H_U - L/(gA)i\omega Q_U \tag{32}$$

Introducing dimensionless variables as: $H = (a'Q_{0r})/(gA')\hat{H}$, $L = L'\hat{x_c}$, $\omega = a'/L'\hat{s}$, and $Q = Q_{0r}\hat{Q}$, the dimensionless lumped inertia can be expressed as follows:

$$\hat{Z_D} = \hat{Z_U} - i\hat{s}\hat{x_c} \tag{33}$$

where $\hat{Z_D}$ and $\hat{Z_U}$ are the dimensionless hydraulic impedances downstream and upstream, respectively.

2.6. Integration of the Dimensionless Response Function with PSO

The objective function needs to be defined to determine the optimum solution for surge tank installation. In this study, two objective functions were used to address the design criteria for different safety standards. The first objective function (OB1) is the minimum pressure head variation at any designated point in the system, which can be defined as follows:

$$\text{OB1} = Minimize\left\{\sum_{i=1}^{n}\left(\hat{h_i} - \hat{h_r}\right)^2\right\} \tag{34}$$

where n is the final time step, $\hat{h_i}$ is the dimensionless pressure head at time step i, and $\hat{h_r}$ is the reference dimensionless pressure head. The other objective function (OB2) considers both the maximum overpressure and minimum underpressure from the reference dimensionless pressure head for a specific point, which can be expressed as follows:

$$\text{OB2} = Minimize\left\{Max\left|\hat{h_i} - \hat{h_r}\right|\right\} \tag{35}$$

In this study, the dimensionless pressure response function was integrated into the PSO scheme [17]. Considering the sensitivity of the surge tank design parameters, three optimizing parameters were selected: the location of the surge tank in the main pipeline, $\hat{x_{dw}}$; the length of the surge tank connector, $\hat{x_c}$; and the ratio of the surge tank cross-sectional area to that of the main pipeline, A_{sr}.

3. Results

An RPSPV system identical to the system used in a previous study [11] was used for the validation of the proposed method (Figure 1). The length of the main pipeline was 150 m with diameters (both main pipeline and surge tank connector) of 0.02 m. The

pipeline length between the downstream valve and surge tank connector was 5 m, and that of the connector was 2 m. The Darcy–Weisbach friction factor of the pipeline elements was 0.03, and the wave propagation speed was 1210.5 m/s. The diameter of the surge tank was 2 m, the steady flow rate from the upstream reservoir to the downstream reservoir was 0.9277×10^{-4} m^3/s, and a water hammer was introduced by rapid closure of the downstream valve, as shown in Figure 1.

3.1. Transient Analysis

Both the developed dimensionless impedance method (DIM) and MOC were used to compute the pressure variations in the pipeline system and validate the proposed method, as shown in Figure 1. The number of grids for the MOC was 300, and its computational time step was 0.00041 s, which satisfied the Courant number of one. To apply the DIM, the maximum frequency for the boundary in the frequency domain integration was 812.28 rad/s and was converted into the maximum dimensionless frequency through the multiplication of L'/a', which equaled 100 rad/unit. The number of fast Fourier transformations required to convert the response function into a dimensionless time domain was 2^{15}. Figure 2 shows well-matched normalized pressure heads at the downstream valve computed by MOC and DIM in the dimensionless time domain, which computed as the multiplication of time with a'/L'. Figure 2 shows the high-frequency surge interaction between the surge tank connector and the downstream end of the main pipeline.

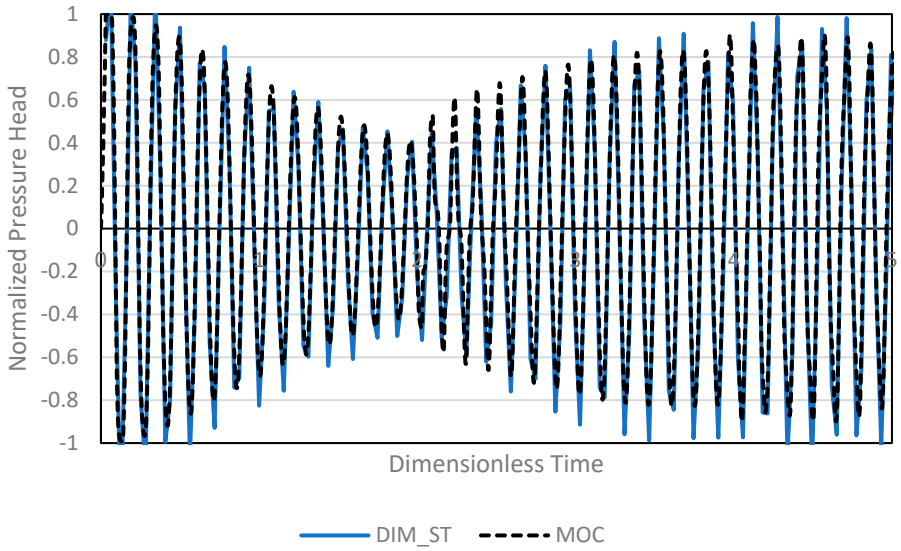

Figure 2. Predictions of normalized pressure head by DIM_ST and MOC at downstream valve.

Pressure head predictions were compared between IRM with surge tank [11] and the DIM method with surge tank (DIM_ST), as presented in Figure 3. Pressure head variations at both the downstream valve (Figure 3) showed perfect matches between the existing IRM and the developed method.

The performances of dimensionless formulations (Equations (28), (29) and (33)) such as lumper inertia as an accumulator, accurate model, and conventional reservoir model for surge tank were compared at the main pipeline connector. Figure 4 shows that differences between three distinct dimensionless formulations were negligible. This indicates that the developed dimensionless approach is a reliable method to simulate hydraulic transient for RPSPV systems.

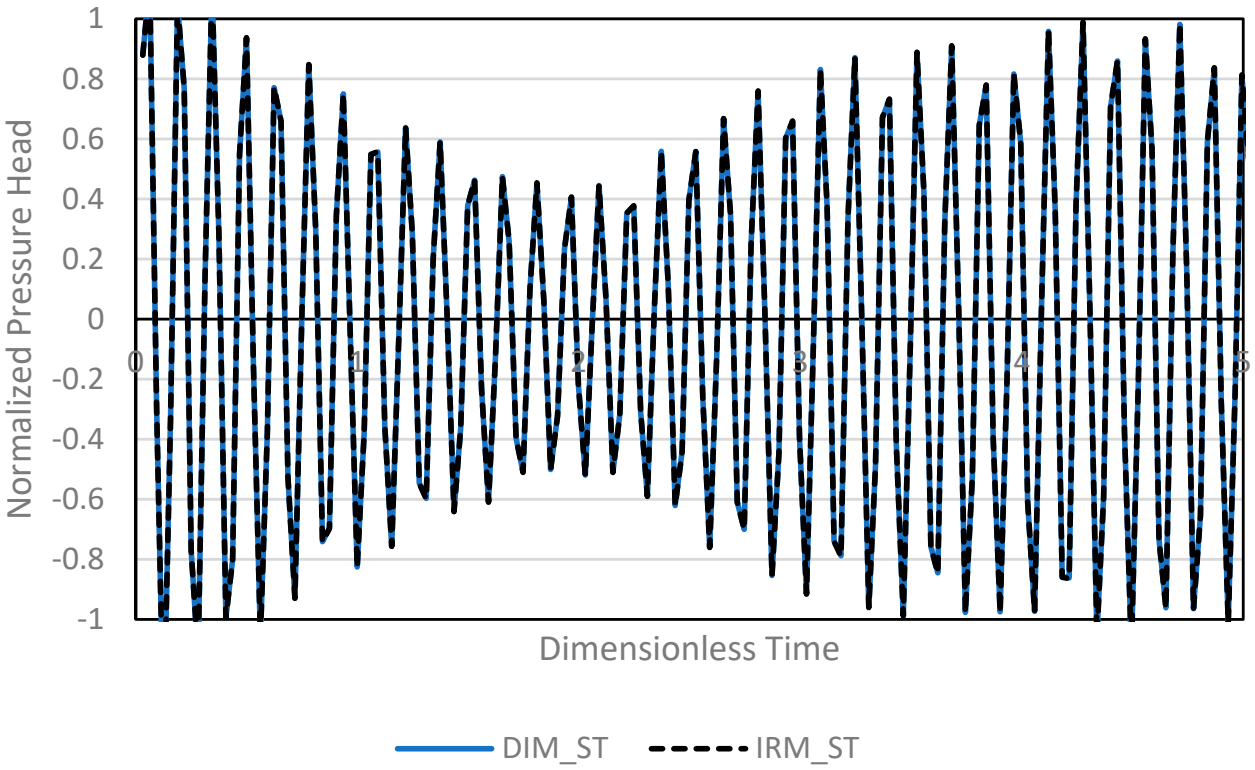

Figure 3. Predictions of normalized pressure head by DIM_ST and the IRM with surge tank (IRM_ST) adapted with permission from Ref. [11] at downstream valve.

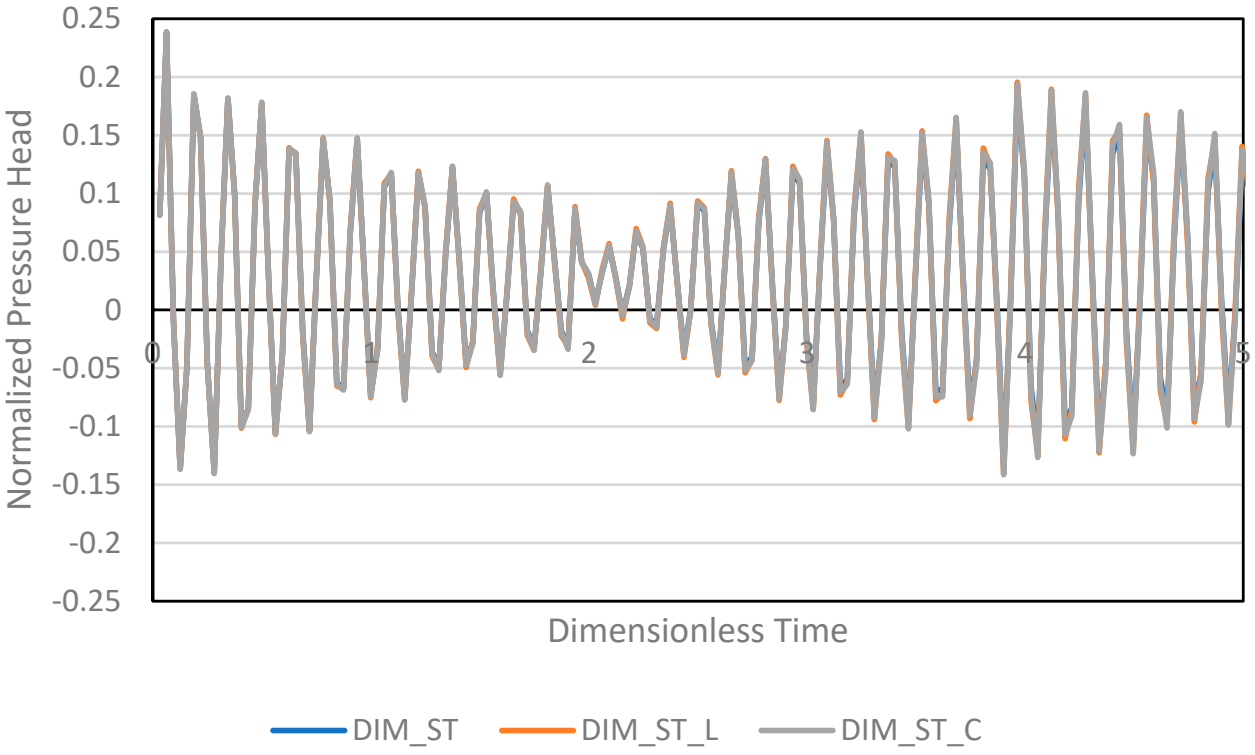

Figure 4. Predictions of normalized pressure head by DIM_ST using Equation (28), the dimensionless lumped inertia (DIM_ST_L) using Equation (33), and the conventional pipeline scheme for the connector (DIM_ST_C) using Equation (29) at the surge tank connector in the main pipeline.

3.2. Optimum Dimensionless Design of RPSPV Systems

The flow regime of RPSPV systems can be comprehensively addressed by the dimensionless resistance (see Equations (5) and (6)), which means that a general design of the RPSPV system can be achieved through the application of the developed method for physically meaningful bounds in $\hat{R}$. Considering the dimensions and materials of pipelines and conventional flow rates in real-life systems, the lower and upper bounds of $\hat{R}$ were specified as 1.25×10^{-7} and 5.4×10^{-4}, respectively. The three most sensitive parameters were selected for the design of the dimensionless RPSPV in a preliminary study [11]. The location of the surge tank in the RPSPV system can be expressed as $x_{\hat{dw}}$. The size of the surge tank is denoted by A_{sr}, and the length of the surge tank connector is denoted by $\hat{x_c}$. The integrated PSO scheme provides optimum solutions for the ranges of $\hat{R}$, which were obtained by 900 iterations for each $\hat{R}$. The water hammer simulation was performed over 80 dimensionless times for each iteration, which is approximately 20 cycles as the theoretical period for the main pipeline element. The upper and lower search bounds for $x_{\hat{dw}}$ were 0.001 and 0.9, and those for A_{sr} and $\hat{x_c}$ ranged from 1 to 20 and 0 to 0.1, respectively.

Table 1 presents optimized dimensionless parameters for the objective function OB1 (Equation (34)) at the downstream valve. The optimization results can be classified into three distinct parts; one is the low resistance part, where $\hat{R}$ is distributed between 1.25×10^{-7} and 1.25×10^{-5}, showing substantially high OB1s. As illustrated in Table 1, the optimum locations of surge tanks were distributed between 0.202 and 0.284 in terms of $x_{\hat{dw}}$, and the dimensionless length of surge tank connectors was 0.08 for the range of low resistance. This means substantial resonances existed not only by the main pipeline surge tank but also by the surge tank connector. Optimized results of parameters in the intermediate range of $\hat{R}$, between 1.25×10^{-4} and 1.69×10^{-2}, showed negligible lengths both for $x_{\hat{dw}}$ and $\hat{x_c}$, which indicates no resonance in any part of the RPSPV system. The high resistance part of $\hat{R}$, between 2.47×10^{-2} and 5.40×10^{-1}, also showed negligible resonance due to small $x_{\hat{dw}}$ and $\hat{x_c}$, but the optimized A_{sr} and OB1 showed an apparent decreasing trend as $\hat{R}$ was increased. The contribution of surge tank area in minimizing OB1 seems to decrease in the higher ranges of $\hat{R}$.

Table 1. Optimized dimensionless parameters for an RPSPV system using an objective function of Equation (34) at the downstream valve.

$\hat{R}$	$x_{\hat{dw}}$	A_{sr}	$\hat{x_c}$	OB1
1.25×10^{-7}	0.202	13.4	0.08	479.7
1.25×10^{-6}	0.202	13.4	0.08	479.5
1.25×10^{-5}	0.284	8.1	0.08	596.2
1.25×10^{-4}	0.001	18.8	0.00	1.4
1.25×10^{-3}	0.001	19.1	0.00	1.4
5.16×10^{-3}	0.001	19.1	0.00	1.3
9.07×10^{-3}	0.001	19.1	0.00	1.3
1.69×10^{-2}	0.001	18.8	0.00	1.3
2.47×10^{-2}	0.001	18.8	0.02	20.8
4.03×10^{-2}	0.001	19.0	0.03	17.0
5.59×10^{-2}	0.001	18.4	0.03	14.3
7.16×10^{-2}	0.001	19.0	0.03	12.3
1.03×10^{-1}	0.001	18.8	0.04	9.7
1.34×10^{-1}	0.009	14.7	0.02	6.6
1.65×10^{-1}	0.001	19.1	0.05	6.9
2.27×10^{-1}	0.009	9.4	0.02	3.9
2.90×10^{-1}	0.009	8.8	0.02	3.1
3.53×10^{-1}	0.009	8.1	0.02	2.5
4.15×10^{-1}	0.009	13.8	0.02	2.2
4.78×10^{-1}	0.001	8.4	0.06	2.7
5.40×10^{-1}	0.001	7.5	0.05	2.4

Optimized dimensionless parameters are presented in Table 2 for objective function OB2 (Equation (35)) at the downstream valve. Table 2 can be divided into two parts: one is the low $\hat{R}$ part, between 1.25×10^{-7} and 1.25×10^{-5}, which shows apparent resonance both in the main pipeline as $x_{\hat{dw}} = 0.693$ and the connector as $\hat{x_c} = 0.03$. The other $\hat{R}$ part, between 1.25×10^{-4} and 5.40×10^{-1}, shows no resonance both in the main pipeline and connector, but only the impact of A_{sr} in minimizing OB2. Both Tables 1 and 2 show the importance of surge tank location as $x_{\hat{dw}}$ for the low resistance regime, where $\hat{R}$ ranges between 1.25×10^{-7} and 1.25×10^{-5}. This is because negligible pressure wave damping under a low resistance condition can introduce resonances showing high-pressure responses even in the later time step. The location of the surge tank can be critical to alleviating water hammer for minimizing the superimposition of peaky resonances both for positive and negative perspectives.

Table 2. Optimized dimensionless parameters for an RPSPV system using an objective function of Equation (35) at the downstream valve.

$\hat{R}$	$x_{\hat{dw}}$	A_{sr}	$\hat{x_c}$	OB2
1.25×10^{-7}	0.693	3.5	0.03	1.58
1.25×10^{-6}	0.693	3.5	0.03	1.58
1.25×10^{-5}	0.693	3.5	0.03	1.58
1.25×10^{-4}	0.001	15.0	0.00	0.03
1.25×10^{-3}	0.001	19.2	0.00	0.03
5.16×10^{-3}	0.001	19.3	0.00	0.03
9.07×10^{-3}	0.001	19.3	0.00	0.03
1.69×10^{-2}	0.001	19.3	0.00	0.03
2.47×10^{-2}	0.001	19.3	0.00	0.03
4.03×10^{-2}	0.001	19.3	0.00	0.03
5.59×10^{-2}	0.001	19.3	0.00	0.03
7.16×10^{-2}	0.001	19.3	0.00	0.03
1.03×10^{-1}	0.001	19.3	0.00	0.03
1.34×10^{-1}	0.001	18.7	0.00	0.03
1.65×10^{-1}	0.001	18.6	0.00	0.03
2.27×10^{-1}	0.001	14.5	0.00	0.03
2.90×10^{-1}	0.001	11.4	0.00	0.03
3.53×10^{-1}	0.001	9.4	0.00	0.03
4.15×10^{-1}	0.001	9.0	0.00	0.03
4.78×10^{-1}	0.001	6.9	0.00	0.03
5.40×10^{-1}	0.001	6.1	0.00	0.03

The desirable location of the surge tank in most pipeline systems appears adjacent to the control valve, indicating that $x_{\hat{dw}}$ can be designated as a very small number, such as 0.001. This means that the optimization of other parameters can be performed using either OB1 or OB2 at the location of the surge tank connector with negligible $x_{\hat{dw}}$. Table 3 presents the optimization results for OB1 at the surge tank connector, which can be divided into two distinct parts. The first is the relatively low $\hat{R}$ part, between 1.25×10^{-7} and 7.16×10^{-2}, which shows no impact of the surge tank connector and a decreasing trend in A_{sr} at higher $\hat{R}$. The other higher range of $\hat{R}$, between 1.03×10^{-1} and 5.40×10^{-7}, shows some resonance in the connector because $\hat{x_c}$ were optimized between 0.03 and 0.04 with the decreasing trend in A_{sr} at higher $\hat{R}$.

Table 3. Optimized dimensionless parameters for an RPSPV system using an objective function of Equation (34) at the surge tank connector.

$\hat{R}$	A_{sr}	$\hat{x_c}$	OB1
1.25×10^{-7}	18.8	0.00	0.0
1.25×10^{-6}	18.8	0.00	0.0
1.25×10^{-5}	18.8	0.00	0.0
1.25×10^{-4}	18.8	0.00	0.0
1.25×10^{-3}	19.2	0.00	0.0
5.16×10^{-3}	19.2	0.00	0.0
9.07×10^{-3}	19.2	0.00	0.0
1.69×10^{-2}	19.2	0.00	0.0
2.47×10^{-2}	12.2	0.00	0.0
4.03×10^{-2}	6.4	0.00	0.0
5.59×10^{-2}	4.2	0.00	0.0
7.16×10^{-2}	3.0	0.00	0.0
1.03×10^{-1}	18.6	0.03	6.2
1.34×10^{-1}	18.7	0.03	4.9
1.65×10^{-1}	18.3	0.04	4.1
2.27×10^{-1}	17.0	0.04	3.1
2.90×10^{-1}	14.1	0.04	2.5
3.53×10^{-1}	11.5	0.04	2.0
4.15×10^{-1}	9.8	0.04	1.8
4.78×10^{-1}	8.9	0.04	1.6
5.40×10^{-1}	7.7	0.04	1.4

Table 4 presents dimensionless parameter optimization results using OB2 at the surge tank connector. No impact of the surge tank connector was observed ($\hat{x_c} = 0$) in all ranges of resistance, and the optimized A_{sr} was changed for $\hat{R}$. The function of A_{sr} in minimizing OB2 at the connector does not appear to be linear to $\hat{R}$, as shown in Table 4.

Table 4. Optimized dimensionless parameters for an RPSPV system using an objective function of Equation (35) at the surge tank connector.

$\hat{R}$	A_{sr}	$\hat{x_c}$	OB2
1.25×10^{-7}	18.9	0.00	0.0
1.25×10^{-6}	18.9	0.00	0.0
1.25×10^{-5}	18.9	0.00	0.0
1.25×10^{-4}	19.0	0.00	0.0
1.25×10^{-3}	19.2	0.00	0.0
5.16×10^{-3}	19.2	0.00	0.0
9.07×10^{-3}	19.2	0.00	0.0
1.69×10^{-2}	19.2	0.00	0.0
2.47×10^{-2}	11.9	0.00	0.0
4.03×10^{-2}	6.3	0.00	0.0
5.59×10^{-2}	4.1	0.00	0.0
7.16×10^{-2}	3.0	0.00	0.0
1.03×10^{-1}	1.9	0.00	0.0
1.34×10^{-1}	1.7	0.00	0.0
1.65×10^{-1}	1.7	0.00	0.0
2.27×10^{-1}	1.7	0.00	0.0
2.90×10^{-1}	1.7	0.00	0.0
3.53×10^{-1}	2.9	0.00	0.0
4.15×10^{-1}	3.9	0.00	0.0
4.78×10^{-1}	18.4	0.00	0.0
5.40×10^{-1}	17.3	0.00	0.0

4. Discussion

The design of surge tanks in pipeline systems has been explored by considering the flow status, dimensions, and fluid properties of a designated system, even though the structural layout (RPSPV) is essentially identical for different pipeline systems. The dimensionless impedance method developed in this study provides generality for modeling the transient and its relaxation impact by the surge tank. A single dimensionless parameter, dimensionless resistance, comprehensively addresses the flow properties (e.g., flow rate and viscosity) as well as the physical features of the pipeline (e.g., length, diameter, friction, and wave speed) for hydraulic transient simulation for any RPSPV system. This means that hydraulic similarity can be achieved if $\hat{R}$ between different RPSPV systems are identical. In other words, the design of a surge relief device can be tested even in a substantially downscaled pipeline system compared with that of the original system through the implementation of identical $\hat{R}$.

The optimization results provide comprehensive surge tank design criteria for RPSPV systems in a universal context. Depending on the objective function and its target position for pressure, Tables 1 and 2 present the impact of resonances in three distinct pipeline elements ($\hat{x_{up}}$, $\hat{x_{dw}}$, and $\hat{x_c}$) as well as the surge energy absorption into the surge tank as A_{sr} for ranges of $\hat{R}$. The impact of high-pressure resonance between pipeline elements was important for low-range dimensionless resistance ($\hat{R}$ = 1.25 × 10^{-7}~1.25 × 10^{-5}). The introduction of a negligible distance between the surge tank location and the downstream valve further simplified the optimization of the dimensionless parameters, as presented in Tables 3 and 4. The distribution of the optimum surge tank size A_{sr}. does not seem to be proportional to $\hat{R}$ (see Tables 3 and 4), indicating that the optimum requirement of surge energy absorption also depends on the flow regime and its pressure amplitude and resonance. The optimization results of the dimensionless parameters (Tables 1–4) can be feasibly applicable to a field pipeline system, as the parameters of the target system were changed into dimensionless terms, which provided efficient parameter identification for the optimum design of the RPSPV system.

5. Conclusions

General surge tank design in pressurized pipeline systems was explored through the development of dimensionless continuity and motion equations. Dimensionless analytical solutions were developed in the dimensionless frequency domain in terms of the general dimensionless relationship between the upstream and downstream dimensionless flow rates and the pressure heads. The flow features of the surge tank connector were implemented in the developed model in terms of the dimensionless propagation constant and characteristic impedance of the connecting pipeline element. Both the hydraulic impedance for the surge tank and lumped inertia as a general description of the accumulator were developed in terms of dimensionless formulations. A series of dimensionless hydraulic impedance formulations were developed from the upstream reservoir to the downstream control valve for the RPSPV system. The solution set of the DIM can be a general guideline for the design of different RPSPV systems, which is simply because the dimensionless solutions can be used for all real-life systems as the conversion for the corresponding system is implemented.

The proposed method was validated through comparisons with existing methods (e.g., the MOC and the IRM), which showed good agreement. Further integration between dimensionless transient modeling and a metaheuristic optimization tool (e.g., PSO) provided comprehensive design guidelines for surge tanks. Depending on the dimensionless resistance, which comprehensively addressed various conditions for hydraulic transients, the optimum design parameters were expressed as surge tank location, connector length, and area. This implies that the similarity in hydraulic transient generation and surge tank impact can be achieved through one matching condition of dimensionless resistance between different RPSPV systems.

In this study, equations and solutions were developed based on the assumption of the steady friction model, which can provide safer results for device design than those obtained from the unsteady friction model. However, the hydraulic transient in complex pipelines can be a more challenging problem because the resonances between many distinct pipeline elements can be extremely complicated. Therefore, further research should be conducted on the implementation of unsteady friction models and diverse pipeline elements (e.g., branches and loops) in the dimensionless modeling of unsteady pipeline flow.

Author Contributions: Conceptualization, S.K.; methodology, S.K.; software, S.K.; validation, S.K. and D.C.; formal analysis, S.K.; writing—original draft preparation, S.K.; writing—review and editing, S.K. and D.C.; project administration, D.C.; funding acquisition, S.K. All authors have read and agreed to the published version of the manuscript.

Funding: This research was funded by K-Water, grant number 21-BT-002.

Institutional Review Board Statement: Not applicable.

Informed Consent Statement: Not applicable.

Data Availability Statement: Not applicable.

Acknowledgments: This research was performed as Project No Open Innovation R&D (21-BT-002) and supported by K-Water.

Conflicts of Interest: The authors declare no conflict of interest.

References

1. Wylie, E.B.; Streeter, V.L. *Fluid Transients in Systems*, 3rd ed.; Prentice-Hall International: London, UK, 1993; pp. 37–79.
2. Di Santo, A.R.; Fratino, U.; Iacobellis, V.; Piccinni, A.F. Effects of free outflow in rising mains with air chamber. *J. Hydraul. Eng.* **2002**, *128*, 992–1001. [CrossRef]
3. Izquierdo, J.; Lopez, P.A.; Lopez, G.; Martinez, F.J.; Perez, R. Encapsulation of air vessel design in a neural network. *Appl. Math. Model.* **2006**, *30*, 395–405. [CrossRef]
4. Martino, G.D.; Fontana, N. Simplified approach for the optimal sizing of throttled air chambers. *J. Hydraul. Eng.* **2012**, *138*, 1101–1109. [CrossRef]
5. Stephenson, D. Simple guide for design of air vessels for water hammer protection on pumping lines. *J. Hydraul. Eng.* **2002**, *129*, 792–797. [CrossRef]
6. Zhou, J.X.; Palikhe, S.; Cai, F.L.; Liu, Y.F. Experimental ad simulation-based investigations on throttle's head loss coefficients of a surge tank. *Energ. Sci. Eng.* **2020**, *8*, 2722–2733. [CrossRef]
7. An, J.F.; Zhang, J.; Yu, X.D.; Chen, S. Influence of flow field on stability of throttled surge tank with standpipe. *J. Hydrodyn.* **2014**, *25*, 292–299. [CrossRef]
8. Guo, W.C.; Liu, Y.; Qu, F.L.; Xu, X.Y. A review of critical stable sectional areas for the surge tanks of hydropower stations. *Energies* **2020**, *13*, 6466. [CrossRef]
9. Kendir, T.E.; Ozdamar, A. Numerical and experimental investigation of optimum surge tank forms in hydroelectric power plant. *Renew. Energy* **2013**, *60*, 323–331. [CrossRef]
10. Wan, W.Y.; Zhang, B.R.; Chen, X.Y.; Lian, J.J. Water hammer control analysis of an intelligent surge tank with spring self-adaptive auxiliary control system. *Energies* **2019**, *12*, 2527. [CrossRef]
11. Kim, S.H. Design of surge tank for water supply systems using the impulse response method with the GA algorithm. *J. Mech. Sci. Technol.* **2010**, *24*, 629–636. [CrossRef]
12. Besharat, M.; Tarinejad, R.; Aalami, M.T.; Ramos, H.M. Study of a compressed air vessel for controlling the pressure surge in water networks: CFD and experimental analysis. *Water Resour. Manag.* **2016**, *30*, 2687–2702. [CrossRef]
13. Boston, M.; Akhtari, A.A.; Bonakdari, H.; Jalili, F. Optimal design for shock damper with genetic algorithm to control water hammer effects in complex water distribution systems. *Water Resour. Manag.* **2019**, *33*, 1665–1681. [CrossRef]
14. Kim, S.G.; Lee, K.B.; Kim, K.Y. Water hammer in the pump-rising pipeline system with an air chamber. *J. Hydrodyn.* **2017**, *26*, 960–964. [CrossRef]
15. Maghaddas, S.M.J.; Samani, H.M.V.; Haghighi, A. Multi-objective optimization of transient protection for pipelines with regard to cost and serviceability. *J. Water Supply Res. Technol.-Aqua* **2017**, *66*, 340–352. [CrossRef]
16. Maghaddas, S.M.J. The steady-transient optimization of water transmission pipelines with consideration of water-hammer control devices: A case study. *J. Water Supply Res. Technol.-Aqua* **2018**, *67*, 556–565. [CrossRef]
17. Kennedy, J.; Eberhart, R. Particle swarm optimization. In Proceedings of the ICNN'95—International Conference on Neural Networks, Perth, Australia, 27 November–1 December 1995. [CrossRef]